IOP Publishing Environ. Res. Lett. 18 (2023) 024026 https://doi.org/10.1088/1748-9326/acb3e2

ENVIRONMENTAL RESEARCH
LETTERS

OPEN ACCESS

RECEIVED
21 September 2022

REVISED
29 December 2022

ACCEPTED FOR PUBLICATION
17 January 2023

PUBLISHED
27 January 2023

LETTER

Air pollution mitigation in North China through flexible heating policies

Jiandong Li[1], **Xin Hao**[1,2,3], **Hong Liao**[1,*], **Huibin Dai**[1], **Nan Li**[1], **Yixuan Gu**[4,5], **Ruijun Dang**[6], **Baojie Li**[1] **and Ying Wei**[7]

[1] Jiangsu Key Laboratory of Atmospheric Environment Monitoring and Pollution Control, Jiangsu Collaborative Innovation Center of Atmospheric Environment and Equipment Technology, School of Environmental Science and Engineering, Nanjing University of Information Science & Technology, Nanjing 210044, People's Republic of China
[2] Collaborative Innovation Center on Forecast and Evaluation of Meteorological Disasters/Key Laboratory of Meteorological Disaster, Ministry of Education, Nanjing University for Information Science & Technology, Nanjing 210044, People's Republic of China
[3] Nansen-Zhu International Research Centre, Institute of Atmospheric Physics, Chinese Academy of Sciences, Beijing 100029, People's Republic of China
[4] Department of Mechanical Engineering, University of Colorado Boulder, Boulder, CO 80301, United States of America
[5] Department of Economics, University of Mannheim, Mannheim, Baden Württemberg 68161, Germany
[6] John A. Paulson School of Engineering and Applied Sciences, Harvard University, Cambridge, MA 02138, United States of America
[7] Institute of Urban Meteorology, China Meteorology Administration, Beijing 100089, People's Republic of China
[*] Author to whom any correspondence should be addressed.

E-mail: hongliao@nuist.edu.cn

Keywords: central heating, PM2.5 pollution, climate change, GEOS-chem, carbon neutrality

Supplementary material for this article is available online

Abstract

Central heating in North China produces severe air pollution, although the need for heating may be reduced by rising temperatures associated with climate change. The regional trend of mean heating length (HL) for North China was −0.32 d per year during 1961–2019. Compared with the 2010–2015 mean values, the start and end dates for central heating in the North China Plain (NCP) during 2050–2055 will delayed by 9 d and advanced by 12 d, respectively, under the Shared Socioeconomic Pathway 5–8.5 (SSP5-85), and by 5 and 8 d under the carbon-neutral (CN) scenario, based on Coupled Model Intercomparison Project phase 6 model simulations. Here we propose a flexible heating policy (FHP), such that HL is determined strictly by temperature, and the associated air pollution benefit of shortening HL are examined by a global 3D chemical transport model GEOS-Chem. The study focused on the year 2019 with the current goal of elimination of severe $PM_{2.5}$ pollution, and with the minimum HL estimated to provide up to a 24% reduction in severe $PM_{2.5}$ pollution (daily mean $PM_{2.5} > 150\ \mu g\ m^{-3}$) over the NCP during periods of FHP implementation. For future CN policies, the NCP can achieve great air quality improvements by 2050, with more than 60% of days throughout the heating season with daily $PM_{2.5}$ concentrations of $<10\ \mu g\ m^{-3}$, and 95% with $<35\ \mu g\ m^{-3}$. Although the SSP5-85 scenario may lead to reduced HLs, pollutant emissions are likely much higher than under CN scenarios, with pollution days of $PM_{2.5} > 100\ \mu g\ m^{-3}$ still occurring frequently by 2050. Our results highlight that FHPs may effectively reduce severe $PM_{2.5}$ pollution, and China's carbon neutrality goals will play critical roles in mitigating air pollution and prolonged heating welfare during future heating season.

1. Introduction

North China is in a central-heating zone because of low temperatures in the boreal winter. The heating period refers the period each year when central-heating systems provide heat to local homes and is also associated with the bulk of residential and industrial energy consumption. Owing to rapid urbanization and population growth, China's energy consumption and emissions from residential central heating have increased dramatically over the last few decades (Zhang *et al* 2020a). As a result, the combustion of fossil fuels for winter heating has become a major air-quality and public-health concern (Xiao *et al* 2015). High $PM_{2.5}$ (particles with an aerodynamic diameter smaller or equal to 2.5 micrometers) exposure and premature mortality in China have been attributed in large part to residential coal combustion in rural areas (Tao *et al* 2018, Zhao *et al* 2018). Previous findings have indicated that winter heating is one of the major causes of China's severe particulate pollution, with heating contributing up to 13.7% of $PM_{2.5}$ emissions in Beijing (Yuan *et al* 2015). The control of residential sector emissions in the Beijing–Tianjin–Hebei region could significantly improve regional $PM_{2.5}$ air quality (Liu *et al* 2016). The promotion of clean-burning fuels in the residential sector could lead to a 13% reduction in national $PM_{2.5}$ emissions and a 12% reduction in premature deaths nationwide (Zhang *et al* 2019). Since 2013, China has introduced the Clean Air Action Plan (2013–2017) and Blue Sky Protection Campaign (2018–2020) to mitigate air pollution, and national annual mean $PM_{2.5}$ concentrations decreased by 32% between 2013 and 2017 owing to regulatory control of power and industry sector emissions. The implementation of residential clean-heating programs also resulted in a rapid decrease in winter $PM_{2.5}$ levels in North China during 2018–2020 (Li *et al* 2021a), indicating that emissions from the residential sector are a major contributor to $PM_{2.5}$ pollution.

The winter heating region of China comprises 15 main provinces, typically referred to as being north of the Qinling–Huaihe Line, where low temperatures are most severe (figure 1). Heating demand is directly influenced by near-surface temperatures, which are sensitive to climate change (Chen *et al* 2021). Previous studies have explored historical and future variations in heating indices, including the Heating Degree Day, the length of heating period (heating length (HL)), the start date for central heating (heating start (HS)), and the end date for central heating (heating end (HE)). Based on daily mean temperatures over 437 stations in China, Shen and Liu (2016) indicated that a later HS and earlier HE have resulted in a reduction in HL of −2.47 d per decade from 1960 to 2011. Chen *et al* (2021) also projected HS would be delayed and HE advanced during 2006–2050 under the future Representative Concentration Pathway (RCP) 4.5 scenario, and HL and Heating Degree Day decreasing by 1.9 °C and 63.2 °C d dec^{-1}, respectively. However, there remain two limitations. First, most previous studies regarding climate-change effects on heating indices placed more emphasis on high-carbon-emission scenarios (i.e. RCP4.5 and RCP8.5). As China is likely to take a low-carbon-emission path after the proposal of the carbon-neutral (CN) policy, it is essential to quantify variations in heating indices under low-carbon-emission scenarios. Second, no previous studies have investigated the associated air-pollution mitigation benefits.

In North China, the heating season is typically from October–November to March–April. Although local governments can decide when heating services start based on local weather conditions, such regulations are not strictly promoted in the central-heating zone in North China. Given that climate change can alter HL substantially, we hypothesize that the implementation of a flexible heating policy (FHP) where the heating period is determined strictly by temperature may achieve significant air pollution reductions. Here we applied the GEOS-Chem model (Bey *et al* 2001) to assess such benefits from two points of view. First, for the current goal of eliminating severe $PM_{2.5}$ pollution before 2025 through the '14th Five-Year Plan', we selected the year with minimum HL during 2013–2020 and evaluated the maximum extent of severe pollution abatement by FHPs. Second, for the future mid-term (2050), changes in HL were estimated using the Coupled Model Intercomparison Project 6 (CMIP6) model under CN and SSP5-85 (shared socioeconomic pathway 5–8.5) (Riahi *et al* 2017), scenarios. Associated air pollution mitigation benefits were investigated.

2. Data and methods

2.1. Near-surface air temperature

CN05.1 gridded daily mean near-surface air temperature data provided by the National Climate Center of China were used, with a spatial resolution of 0.25° × 0.25° for the years 1961–2020 (Wu and Gao 2013). CN05.1 datasets were derived by interpolation of data from 2416 observation stations in China and have been widely used in studies of climate extremes including extreme precipitation (He *et al* 2021) and heatwaves (Wang *et al* 2022). Future climate simulation data for near-surface air temperatures were derived from 35 CMIP6 models (table S1). All model outputs were interpolated into a common 2.5° × 2.5° grid using the bilinear interpolation method (Li *et al* 2021b). Projections under SSP5-85 and SSP1-26 were considered as representing high carbon emission and carbon neutrality, respectively.

2.2. HS and HE

Beijing's central-heating regulations indicate that if the temperature is below 5 °C for five consecutive days, heating can be started (http://service.law-star.com/cacnew/201011/440067099.htm). Accordingly, HS denotes the last date of the period when the daily mean temperature is <5 °C for five consecutive days, and HE is the last date when the mean temperature is >5 °C for five consecutive days for the first time during the following year. HL is thus determined by HS and HE.

2.3. GEOS-chem model

Air quality over the North China Plain (NCP) during the heating season was simulated using the GEOS-Chem model (version 11.1; http://acmg.seas.harvard.edu/geos/) driven by the US NASA Modern-Era Retrospective Analysis for Research and Applications, Version 2 (MERRA-2), with meteorological data from NASA's Global Modeling and Assimilation Office (GMAO) (Gelaro *et al* 2017). The nested-grid capacity of GEOS-Chem over Asia (11°S–55°N, 60°–150°E) was used with a horizontal resolution of 0.5° latitude by 0.625° longitude and 47 layers up to an altitude of 0.01 hPa. Boundary conditions for gases and aerosols were updated every 3 h from coupled global GEOS-Chem simulations performed at 2° × 2.5° horizontal resolution. $PM_{2.5}$ concentrations were calculated as the sums of simulated mass concentrations of sulfate, nitrate, ammonium, black carbon (BC), and organic carbon (OC) (Dang and Liao 2019).

2.4. Residential emissions

For anthropogenic emissions, the Multi-resolution Emission Inventory of China (MEIC, http://meicmodel.org) was used (Li *et al* 2017a, Zheng *et al* 2018), and the MIX (a mosaic anthropogenic emission inventory over Asia) emission inventory (Li *et al* 2017b) was used for rest domains. For projected anthropogenic emissions in 2050, the Dynamic Projection for Emission in China (DPEC) was obtained (Tong *et al* 2020). The DPEC was developed to explore China's future anthropogenic emission pathways and had integrated the energy system model, emission inventory model, dynamic projection model, and parameterized scheme of Chinese policies. Compared to CMIP6 emissions, the DPEC are more accurate in predicting future variations in emissions of China due to a comprehensive consideration of detailed local environmental and climate policies. All three emissions (MEIC, MIX, and DPEC) inventories provide monthly anthropogenic emissions of major gaseous and particulate pollutants from industry, transport, power, agriculture, and residential sectors. Monthly emissions of total BC, OC, nitrogen oxides (NOx), sulfur dioxide (SO_2), carbon monoxide (CO), and primary $PM_{2.5}$ in the NCP from the residential sector are compared in figure S1 for different scenarios. During the NCP heating season, emissions from the residential sector increase sharply owing to coal combustion for central heating, whereas variations in emissions are minimal during the non-heating season (figure S1). For each simulation (section 2.5), residential emissions outside the central-heating period were considered as those averaged over the non-heating season.

2.5. Numerical experiments

GEOS-Chem simulations were undertaken for the NCP, where $PM_{2.5}$ pollution is most severe (Li *et al* 2019). The beneficial effects of the FHP were considered from two points of view. First, given the change in HL during 2013–2020 when severe $PM_{2.5}$ pollution events were common, we assessed the impact of the FHP on severe air pollution through two experiments: (a) the Base_19 experiment with air-quality simulations under the fixed heating policy of 2019, from November 15, 2019, to March 15, 2020; (b) the FHP_19 experiment with air-quality simulations under the FHP where HS and HE were determined by air temperature. The year 2019 was chosen because it had the minimum HL for 2013–2020 (figure S2), indicating maximum benefit of the FHP. Second, future benefits were quantified under CN and SSP5-85 scenarios through four experiments: the Base_13, Base_17, FHP_CN, and FHP_SSP5-85 experiments. The Base_13 and Base_17 experiments were configured as for Base_19, but for the years 2013 and 2017, respectively. In the FHP_CN and FHP_SSP5-85 experiments, future changes in HL were determined using daily near-surface air temperatures from CMIP6 models under the SSP1-26 and SSP5-85 scenarios, respectively. Projected anthropogenic emissions in 2050 were provided by the DPEC emission inventory. In the FHP_CN and FHP_SSP5-85 scenarios, 2013 and 2017 were assumed to have stagnant and favorable meteorology, respectively, with anthropogenic emissions and stagnant weather conditions in the NCP both impacting $PM_{2.5}$ pollution levels. Earlier studies have shown that severe $PM_{2.5}$ pollution events occurred most frequently in 2013, and that both mean $PM_{2.5}$ concentrations and the frequency of severe $PM_{2.5}$ pollution events were at their lowest during the winter of 2017 (Li *et al* 2018, 2019, Zhang *et al* 2019, 2020b, Li *et al* 2022). Model configurations for the different experiments are shown in table 1.

2.6. Statistical methods

Ground-based $PM_{2.5}$ measurements undertaken by the China Ministry of Ecology and Environment (http://106.37.208.233:20035/) at 39 observation cities in the NCP were used to assess model performance in simulating $PM_{2.5}$ concentrations (figure 1). Following the quality control criterion in a previous study (Li *et al* 2019), the original hourly data were processed to daily time series for each city. The performance of the WRF-Chem model was assessed using the correlation coefficient (R), normalized mean bias (NMB), and index of agreement (IOA). The IOA is a scale of 0–1 that indicates how close model results and observations are to being in perfect agreement. In general, the performance of the model is excellent if R and IOA are close to 1 and NMB is close to 0. Moreover, the Bland–Altman approach (Bland and Altman 1986) is used to assess the difference between simulation and observation within 95% limits of agreement of the mean difference (1.96 of the standard deviation). The Bland–Altman plot

Table 1. HS and HE settings for each experiment.

Experiment	Heating period	Anthropogenic emissions	Meteorological fields
Base_19	15 November–15 March, 2019	MEIC-2019	2019
FHP_19	23 November–5 March, 2019	MEIC-2019	2019
Base_13	15 November–15 March, 2013	MEIC-2013	2013
Base_17	15 November–15 March, 2013	MEIC-2017	2017
FHP_CN	20 November–7 March, 2013	DPECv1.1, Ambitious-pollution-Neutral-goals	2013
	20 November–7 March, 2017	DPECv1.1, Ambitious-pollution-Neutral-goals	2017
FHP_SSP5-85	24 November–3 March, 2013	DPECv1.0, SSP5-85-BHE	2013
	24 November–3 March, 2017	DPECv1.0, SSP5-85-BHE	2017

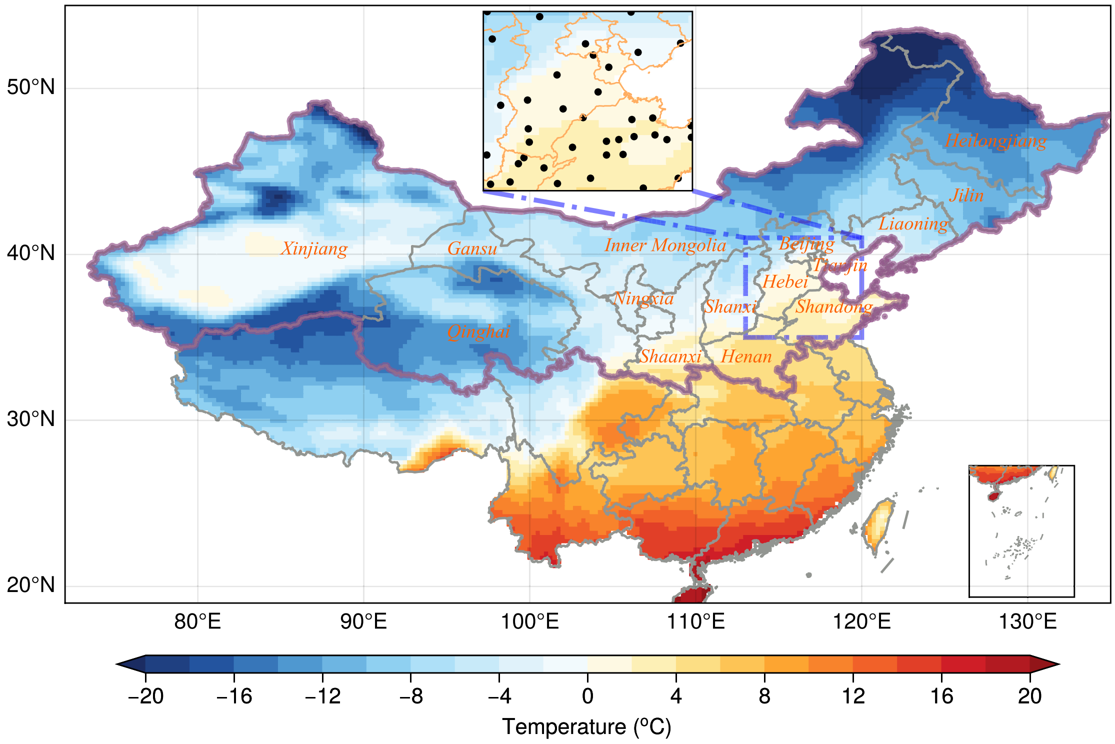

Figure 1. Spatial distribution of mean near-surface air temperature during the heating season (November–March) for 1961–2020. The purple boundary indicates the central heating zone comprising 15 provinces, the inset denotes the North China Plain, and black dots are major cities with $PM_{2.5}$ observations.

illustrates the difference (y-axis) as a function of the average (x-axis), allowing additional information to be presented about the error structure. Metric formulae are as follows:

$$R = \frac{\sum_{i=1}^{N}(M_i - \bar{M})(O_i - \bar{O})}{\sqrt{\sum_{i=1}^{N}(M_i - \bar{M})^2 \sum_{i=1}^{N}(O_i - \bar{O})^2}}$$

$$NMB = \frac{\sum_{i=1}^{N}(M_i - O_i)}{\sum_{i=1}^{N}O_i} \times 100\%$$

$$IOA = 1 - \frac{\sum_{i=1}^{N}(M_i - O_i)^2}{\sum_{i=1}^{M}(|M_i - \bar{O}| + |O_i - \bar{O}|)^2}$$

where M_i and O_i denote simulated and observed $PM_{2.5}$ concentrations, respectively; N indicates the total number of daily samples compared; and $\bar{M}$ and $\bar{O}$ represent averaged simulations and observations, respectively.

3. Results

3.1. Historical changes in HS, HE, and HL

Long-term trends in HS and HE for 1961–2020 are shown in figures 2(a) and (b). The increasing trends of HS indicate a marked delay of central heating in most regions of North China since the 1960s, particularly in Qinghai (0.4–0.5 d per year) and, to a lesser extent, NE China and Xinjiang Province (0.1–0.3 d per year). The regional mean trends in HS for North China and the NCP were 0.14 and 0.06 d per year, respectively. Regarding HE, almost the entire North China region exhibited significant advances with negative trends in central North China of −0.2 to −0.4 d per year. The regional mean trends in HE for North China and the NCP were −0.19 and −0.25 d per

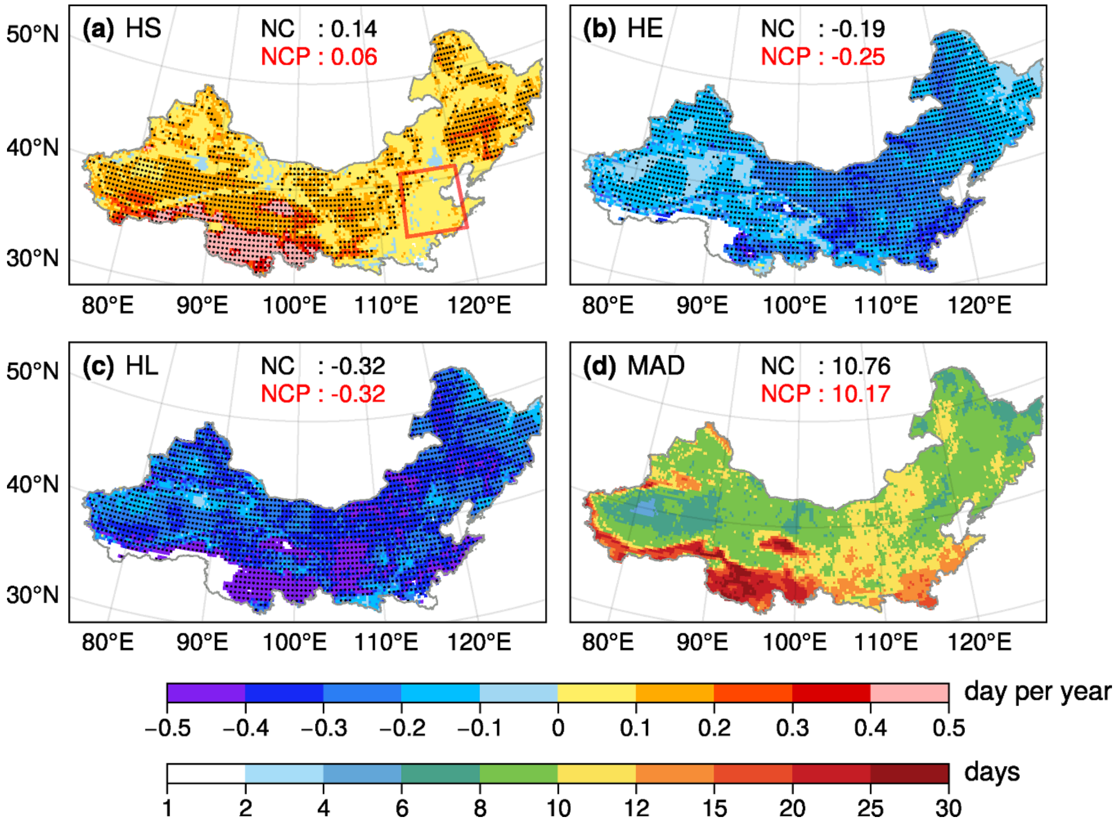

Figure 2. Spatial distributions of annual trends for (a) HS, (b) HE, (c) HL, and (d) mean absolute deviation (MAD) in North China during 1961–2020. Regional mean trends of HS, HE, HL, and MAD for North China (NC) and the North China Plain (NCP) are indicated. Statistical significance above the 95% confidence level based on a Student's *t*-test is indicated as black stippling in panels (a)–(c).

year, respectively, with greater reductions than for HS. Overall, all 15 northern provinces exhibited consistent variations with delay of HS and advance of HE, consistent with the findings of previous studies (Shen and Liu 2016, Chen *et al* 2021). The heating season generally started in October–November and ended in March–April. HS and HE are thus dominated respectively by autumnal and spring temperatures (Chen *et al* 2021). We investigated the long-term trends in surface temperature from 1960 to 2020 for spring, summer, autumn, and winter. Spring warming trends were generally more marked than those of autumn (figure S3), possibly explaining why the linear trend in HE is steeper than that in HS. The whole of North China displayed a significant reduction in HL from 1960 to 2019 (figure 2(c)), indicating the influence of global warming. The regional mean trend of HL in the NCP was −0.32 d per year from 1961 to 2019. We also examined the mean absolute deviation (MAD) in HL, which has received little attention in previous studies. Interannual variations in HL have a varied distribution across North China, with a highest MAD value of 25–30 d in southern Qinghai Province and the Hexi Corridor. For the NCP, the regional mean MAD was approximately 10 d.

Changes in HS and HE during 2011–2020 are compared with changes during 1961–1970 in figure S4. Over the central-heating zone, regions with earlier HS are mainly those north of Heilongjiang Province and the Qinghai Plateau, where heating is required as early as the beginning of October (figure S4(a)). The regions with early HS typically correspond to those with late HE, which occurs at around the end of April (figure S4(b)). During 2011–2020, HS for the NCP was delayed to the last ten days of November, and HE was brought forward to before March 15, which is the current official HE. Compared with 1961–1970, the regional mean HL in the NCP decreased by 15.8 d during 2011–2020. These results indicate the flexibility of the duration of heating over the NCP.

3.2. Future projections of heating period

Future changes in HS and HE under a CN scenario are indicated in figure 3. Climate change may substantially alter HL by delaying HS and advancing HE in the future medium-term (2050–2055) relative to the historical period of 2010–2015. The most significant delay of HS may occur in the southern Qinghai province (figure 3(a)), with a maximum delay of 15–20 d. The spatial pattern of likely changes in HE in North China is similar to that of HS, except that the greatest changes occur in southern Shandong and Henan provinces. For the NCP, the latest HS is projected to be later than December 1

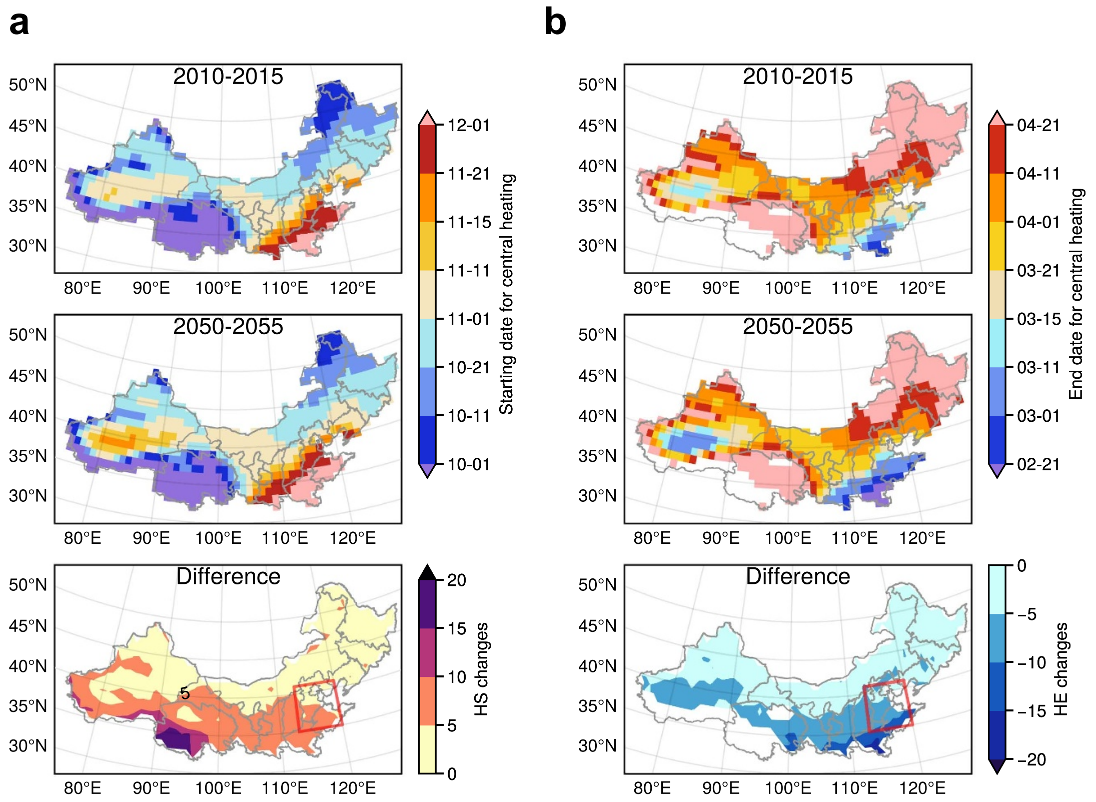

Figure 3. Changes of (a) HS and (b) HE for central heating in North China for 2010–2015 and 2050–2055 under the carbon-neutral scenario.

during 2050–2055, and the earliest HE before March 11. Spatial changes in HS and HE are similar under the SSP1-26 and SSP5-85 scenarios, but with larger magnitudes in the latter (figure S5). Averaged over the whole NCP, HS and HE changes are estimated to be 5 and 8 d under a CN scenario, and 9 and 12 d under an SSP5-85 scenario, respectively. These changes are considered in future simulation by the GEOS-Chem model (table 1).

3.3. Air pollution mitigation with a FHP

Here we first evaluate model performances in the reproduction of $PM_{2.5}$ spatial patterns and temporal evolutions in the Base_13, Base_17, and Base_19 experiments. Spatial distributions of simulated and observed average near-surface $PM_{2.5}$ concentrations for November–March in 2013, 2017, and 2019 in the NCP are shown in figure 4(a). In 2013, the simulated average near-surface $PM_{2.5}$ concentrations exceeded 100 μg m^{-3} over large areas of the NCP. The underestimation over the western NCP is likely due to the coarse spatial resolution of GEOS-Chem (0.5° × 0.625°), which cannot properly resolve the complex topography of the Taihang mountains (Long *et al* 2016). Since 2013, anthropogenic emissions have decreased substantially through clean-air actions (Zhang *et al* 2019). In 2017 and 2019, the simulated mean $PM_{2.5}$ concentrations were much lower than in 2013. Overall, the simulated $PM_{2.5}$ distributions were generally consistent with observations, albeit with slight model biases. The temporal evolution of simulated and observed near-surface $PM_{2.5}$ concentrations is described in figure 4(b). The model generally performed well in reproducing temporal variations in $PM_{2.5}$ concentration in the NCP, with R and IOA values of 0.82 and 0.89, 0.65 and 0.79, and 0.73 and 0.85 for 2013, 2017, and 2019, respectively. $PM_{2.5}$ concentrations were slightly underestimated relative to 2013 observations, with an NMB value of −8.17%. In contrast, $PM_{2.5}$ concentrations were overestimated for 2017 and 2019, with NMB values of 12.51% and 4.17%, respectively. The statistical performances of R, NMB and IOA exceeded the benchmark of modeling performance of daily $PM_{2.5}$ in China ($R > 0.6$, $NMB < 20\%$ and $IOA > 0.7$) (Huang *et al* 2021), indicating that the three base experiments captured $PM_{2.5}$ variations well during the heating season, thereby providing confidence for further analysis. According to the Bland–Altman analysis (figure S6), more than 95% (146/152, 145/152 and 145/152 for 2013, 2017 and 2019) of the differences between simulated and observed $PM_{2.5}$ concentrations lie between the 95% limits of agreement (1.96 of the standard deviation), indicating that the daily $PM_{2.5}$ concentrations from Geos–Chem simulation and observations are consistent with one another.

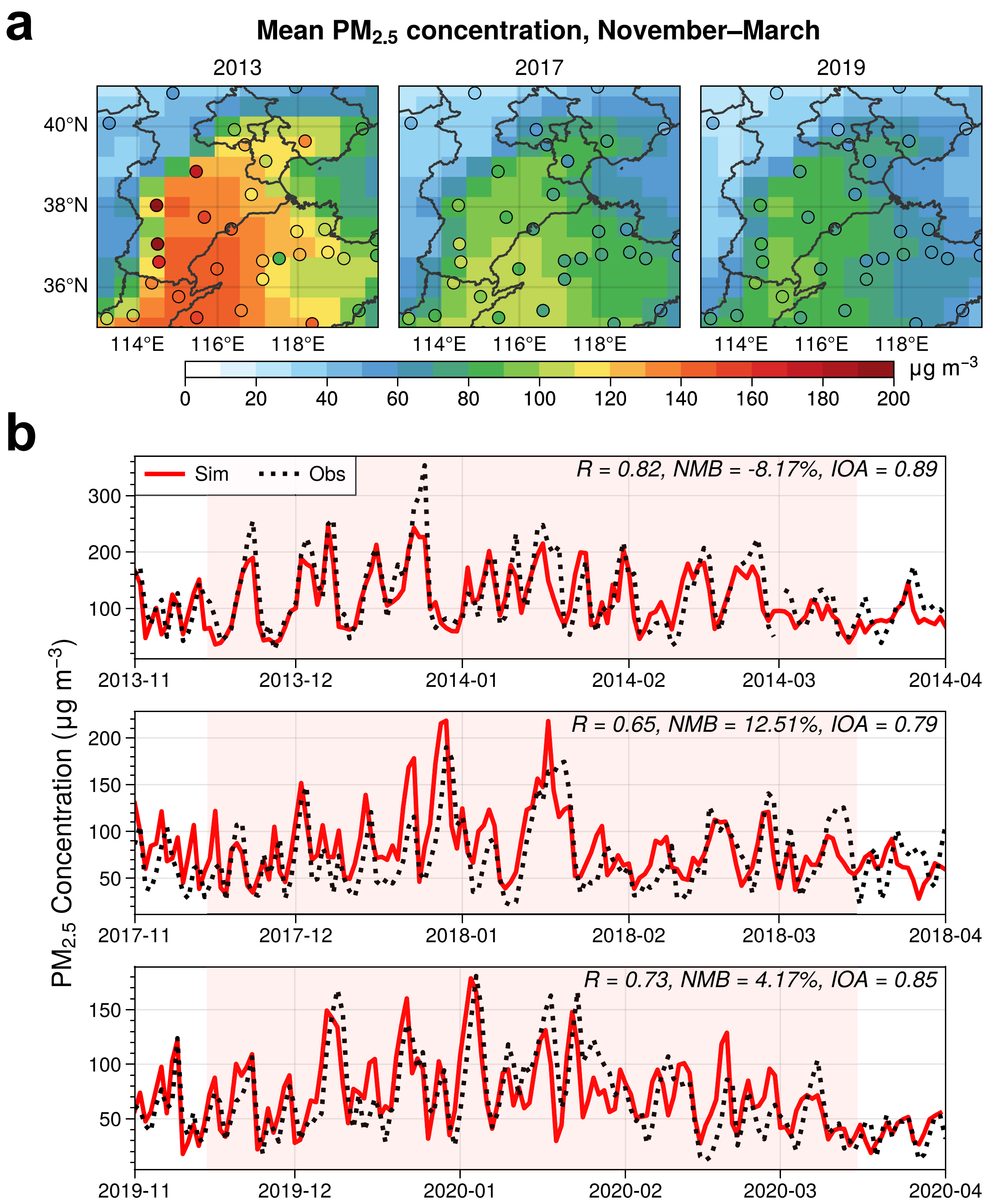

Figure 4. (a) Spatial distribution of simulated (Sim) and observed (Obs) near-surface $PM_{2.5}$ concentrations (shading and colored circles, respectively) averaged from November to March the following year. (b) Comparison of observed and simulated (black dots and solid red lines, respectively) near-surface daily $PM_{2.5}$ concentrations averaged over monitoring sites (circles shown in (a)) for November–March. Pale red shadings indicate current central-heating periods in the NCP (November 15 to March 15).

The mean biases (95% limits of agreement) were—10.0 μg m^{-3} (–79.4 and 59.4), 9.2 μg m^{-3} (–50.2 and 68.5), and 2.8 μg m^{-3} (–47.7 and 53.3) for 2013, 2017 and 2019, respectively.

Differences in mean $PM_{2.5}$ concentrations and number of severe $PM_{2.5}$ pollution days (SPPDs) between the Base_19 and FHP_19 experiments during heating adjustment periods (15–22 November, 2019, and 6–15 March, 2020) are compared in figure 5. Southern Hebei province had the greatest improvement in air quality, with daily mean $PM_{2.5}$ concentrations decreasing by as much as 9 μg m^{-3}. The adoption of FHPs effectively reduced the risk of SPPDs. When the entire NCP was taken into account, the number of SPPDs decreased from 79 to 60 d, a reduction of almost 24%. The '14th Five-Year Plan' for ecological and environmental protection now includes the elimination of severe pollution as a target for several cities in North China by the year 2025. Our findings imply that encouragement of FHPs may aid accomplishment of this objective.

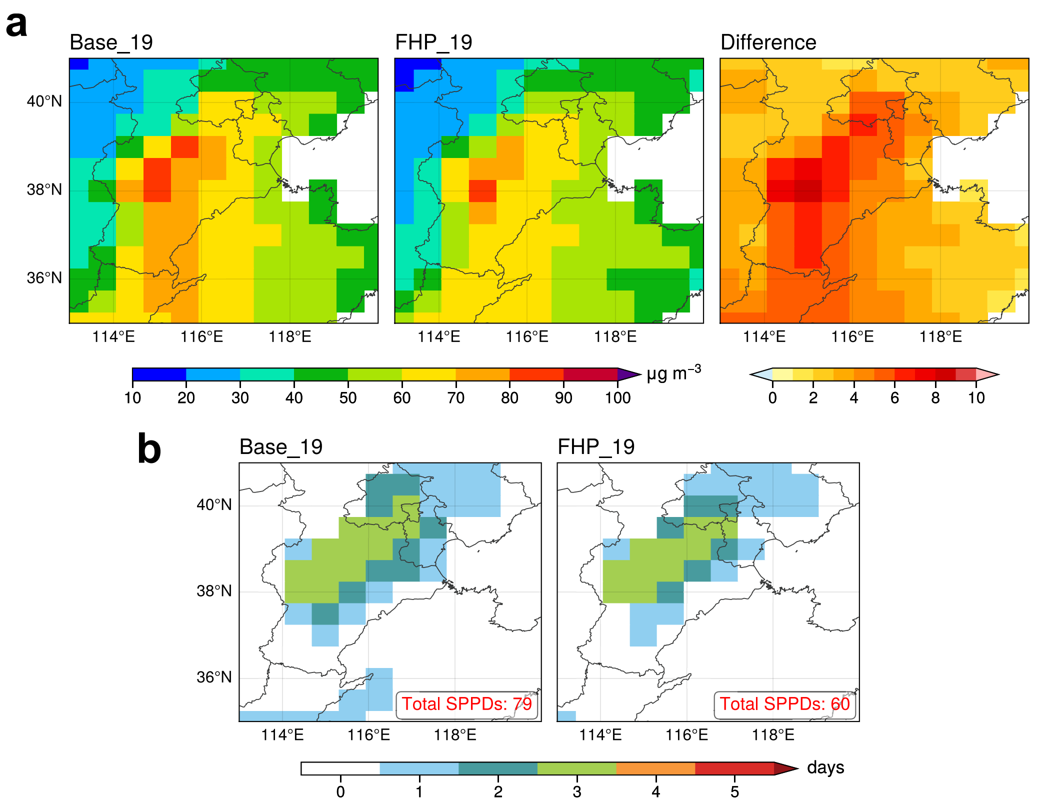

Figure 5. (a) Spatial distribution of mean $PM_{2.5}$ concentrations over the adjusted heating policy periods of 2019 for the Base_19 and FHP_19 experiments, and their difference, respectively. (b) As for (a), but for the total frequency of severe $PM_{2.5}$ pollution days (SPPDs).

Differences in $PM_{2.5}$ concentrations between the FHP_CN and FHP_SSP5-85 scenarios during the future heating season (November 15 to March 15, 2050) are shown in figure 6. In the FHP_CN experiment, there was a significant improvement in air quality, with a mean $PM_{2.5}$ concentration of <20 $\mu g\ m^{-3}$ during the heating season in the NCP. Mean $PM_{2.5}$ concentrations under the SSP5-85 scenario were much higher, even though the HL was lower. The highest $PM_{2.5}$ concentrations, exceeding 35 $\mu g\ m^{-3}$, were in the Beijing area. In the FHP_CN experiment, areas with high $PM_{2.5}$ concentrations also experienced a noticeable improvement in air quality. For example, the mean $PM_{2.5}$ concentration during the heating season was reduced by up to 30 $\mu g\ m^{-3}$ in the northern NCP. Averaged over the whole NCP, mean $PM_{2.5}$ concentrations during the heating season ranged from 8.1 to 10.0 $\mu g\ m^{-3}$ and from 18.4 to 22.6 $\mu g\ m^{-3}$ under the CN and SSP5-85 scenarios (figure 6(b)), respectively. The $PM_{2.5}$ concentration under the CN scenario was about half that under the SSP5-85 scenario due to variations in anthropogenic emissions. The emissions for major pollutants, including BC, OC, NOx, SO_2, CO, and primary $PM_{2.5}$, decreased more dramatically under a CN scenario in 2050 relative to a SSP5-85 scenario (figure S7). No SPPDs were detected during the heating season of 2050. However, high probabilities of pollution days with daily $PM_{2.5}$ exceeding 100 $\mu g\ m^{-3}$ remain for the SSP5-85 scenario. Under the CN scenario, high air quality would be realized on >60% of days throughout the heating season with daily $PM_{2.5}$ concentrations of <10 $\mu g\ m^{-3}$, and on 95% of days with concentrations of <35 $\mu g\ m^{-3}$ (figure 6(c)). The CN scenario may thus have a substantial positive impact on human health through reductions in $PM_{2.5}$ pollution, although more effort would be required to reduce $PM_{2.5}$ concentrations to the new World Health Organization recommended value of 5 $\mu g\ m^{-3}$ (World Health Organization 2021).

4. Discussion and implications

There are inevitably various uncertainties and limitations in our investigation. First, future near-surface air temperature projections under the SSP1-26 scenario do not strictly match CN goals. We used future climate data from SSP1-26 (involving 35 models) because insufficient data were available under SSP1-19 (using only 15 models) in CMIP6. The CO_2 emission pathway under China's ambitious carbon neutrality goals was found to lie between those of SSP1-26 and SSP1-19 when compared with global climate predictions (Cheng *et al* 2021). Therefore, the surface temperature under SSP1-26 is expected to be slightly higher than that under the CN scenario, with

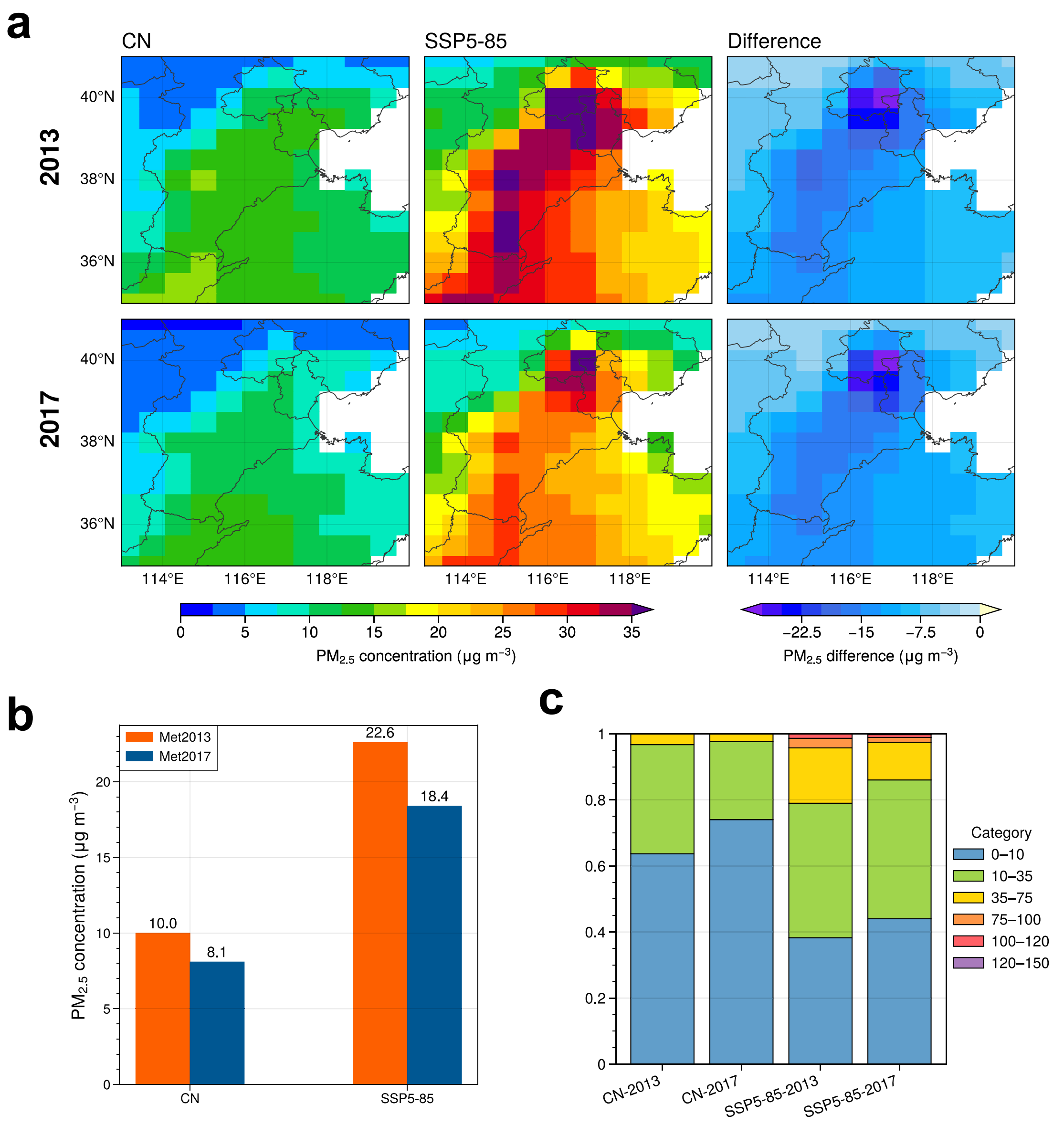

Figure 6. (a) Spatial distribution of mean $PM_{2.5}$ concentration during the heating period (November 15 to March 15) under the CN and SSP5-85 scenarios for 2013 and 2017. (b) Mean $PM_{2.5}$ concentration and (c) its frequency distribution in the NCP during the heating period under the CN and SSP5-85 scenarios for 2013 and 2017.

future changes in HL possibly being overestimated. Second, there also existed biases from input emission. The relatively poor performance in 2017 may be attributed to the uncertainty from emission inventories. During the winter of 2017, the Chinese government implemented stringent emission controls to achieve the goal of Air Pollution Prevention and Control Action Plan, which started in 2013 and the first phase of plan ended in 2017. The residential emissions for the adjusted non-heating days during heating periods were configured roughly as averages over the non-heating season (April–October), which may lead to uncertainties. Third, unique changes in HS and HE were taken into account for the entire NCP in model simulations, resulting in uncertainties for subregions. The spatial distributions of future changes for both HS and HE are not uniform over the NCP, with southern NCP areas exhibiting larger changes than the northern NCP (figure S6). Changes in HL were thus under- and over-estimated for the southern and northern NCP, respectively.

This study investigated $PM_{2.5}$ pollution reduction through implementation of FHPs in the contexts of current and future climate-change scenarios, with two suggestions arising for air-quality improvement during the heating season in North China. First, the promotion of FHP may aid achievement of the goal of eliminating severe $PM_{2.5}$ pollution by 2025. Our analysis indicates that an FHP may lead to a 24% reduction in severe $PM_{2.5}$ pollution over the NCP. In addition to air-quality improvement, the FHP is also expected to reduce mortality risks caused by exposure to highly polluted environments. Second, the government should follow the CN scenario to promote further air-quality improvement. Emissions of major air pollutants (BC, OC, SO_2, NOx, and $PM_{2.5}$) will decline sharply under the CN pathway (figure S7), and the national mean $PM_{2.5}$ concentration would be below 10 $\mu g\ m^{-3}$ by 2060 as a consequence of clean energy structures and strict clean-air policies (Cheng *et al* 2021), with HL variations barely affecting air quality and allowing longer heating periods for public welfare.

5. Conclusion

During the heating season of the boreal winter, increasing coal consumption due to central heating is one of the primary causes of severe $PM_{2.5}$ pollution in North China. Given the causal relationship between air temperature and HL, increased near-surface air temperatures during climate change is likely to shorten HL in North China. It is therefore essential to quantify the air quality benefit under different climate scenarios in order to guide future central heating policy. Based on daily temperature observations during 1961–2020 and outputs of the CMIP6 climate model for 2020–2050, historical and future changes in three heating indices (HS, HE, and HL) were assessed. The GOES-Chem model was used to evaluate the benefits to air quality of promoting FHPs under various climate-change scenarios.

The results indicate that HL over North China decreased during 1961–2020 owing to delayed HS and advanced HE. Changes in HE made the greatest contribution because of the increasing spring warming rate. For the most polluted NCP, the regional mean HL decreased by 15.8 d during 2011–2020 relative to 1961–1970. Interannual variations in HL in the NCP ranged from 8 to 12 d, indicating potential for pollution abatement through FHPs. A GEOS-Chem simulation for 2019 with minimum HL indicated a 24% reduction in SPPDs over the NCP during FHP implementation periods.

With future climate warming, HL in the NCP will continue to decrease during 2020–2050. Relative to 2010–2015, changes in HS and HE during 2050–2055 are projected to respectively be delayed and advanced by 5 and 8 d under the CN scenario, and by 9 and 12 d under the SSP5-85 scenario. Adoption of these changes into the heating period for 2050 yielded simulated mean $PM_{2.5}$ concentrations of 8.1–10.0 and 18.4–22.6 $\mu g\ m^{-3}$ under the under CN and SSP5-85 scenarios, respectively. High risks of pollution days remain with daily $PM_{2.5}$ of $>100\ \mu g\ m^{-3}$ under SSP5-85, but improved air quality should be realized on more than 60% of days throughout the heating season with daily $PM_{2.5}$ concentrations of $<10\ \mu g\ m^{-3}$, and 95% with $<35\ \mu g\ m^{-3}$, under the CN scenario. We recommend adoption of the future CN pathway for achievement of both air-quality improvement and heating welfare, despite the warming scenario of SSP5-85 reducing more HL. Our findings may guide further implementation of heating policy in North China.

Data availability statement

Hourly $PM_{2.5}$ observations were obtained from http://106.37.208.233:20035/. The MERRA-2 reanalysis meteorological data can be accessible through https://gmao.gsfc.nasa.gov/reanalysis/MERRA-2/. CMIP6 outputs are available from https://esgf-node.llnl.gov/search/cmip6/.

The data that support the findings of this study are openly available at the following URL/DOI: https://esgf-node.ipsl.upmc.fr/search/cmip6-ipsl/.

Code availability

The GEOS-Chem model code can be downloaded from http://acmg.seas.harvard.edu/geos/.

Acknowledgments

This research has been supported by the National Key Research and Development Program of China (Grant No. 2019YFA0606800), the National Natural Science Foundation of China (Grant No. 42293320), and the Carbon Peak Carbon Neutral Science and Technology Innovation Foundation of Jiangsu Province (Grant No. BK20220031).

Conflict of interest

The authors declare that they have no conflict of interest.

References

Bey I, Jacob D J, Yantosca R M, Logan J A, Field B D, Fiore A M, Li Q, Liu H Y, Mickley L J and Schultz M G 2001 Global modeling of tropospheric chemistry with assimilated meteorology: model description and evaluation *J. Geophys. Res. Atmos.* **106** 23073–95

Bland J M and Altman D 1986 Statistical methods for assessing agreement between two methods of clinical measurement *Lancet* **327** 307–10

Chen Y, Guo J, Yuan S and Hu C 2021 Effects of climate change on the heating indices in central heating zone of China *Build. Environ.* **195** 107743

Cheng J *et al* 2021 Pathways of China's $PM_{2.5}$ air quality 2015–2060 in the context of carbon neutrality *Natl Sci. Rev.* **8** nwab078

Dang R and Liao H 2019 Severe winter haze days in the Beijing–Tianjin–Hebei region from 1985 to 2017 and the roles of anthropogenic emissions and meteorology *Atmos. Chem. Phys.* **19** 10801–16

Gelaro R *et al* 2017 The modern-era retrospective analysis for research and applications, Version 2 (MERRA-2) *J. Clim.* **30** 5419–54

He L, Hao X, Li H and Han T 2021 How do extreme summer precipitation events over eastern china subregions change? *Geophys. Res. Lett.* **48** e2020GL091849

Huang L *et al* 2021 Recommendations on benchmarks for numerical air quality model applications in China—Part 1: $PM_{2.5}$ and chemical species *Atmos. Chem. Phys.* **21** 2725–43

Li C, Hammer M S, Zheng B and Cohen R C 2021a Accelerated reduction of air pollutants in China, 2017–2020 *Sci. Total Environ.* **803** 150011

Li J *et al* 2022 Winter particulate pollution severity in North China driven by atmospheric teleconnections *Nat. Geosci.* **15** 349–55

Li J, Hao X, Liao H, Hu J and Chen H 2021b Meteorological impact on winter $PM_{2.5}$ pollution in Delhi: present and future projection under a warming climate *Geophys. Res. Lett.* **48** e2021GL093722

Li J, Liao H, Hu J and Li N 2019 Severe particulate pollution days in China during 2013–2018 and the associated typical weather patterns in Beijing–Tianjin–Hebei and the Yangtze River Delta regions *Environ. Pollut.* **248** 74–81

Li K, Liao H, Cai W and Yang Y 2018 Attribution of anthropogenic influence on atmospheric patterns conducive to recent most severe haze over Eastern China *Geophys. Res. Lett.* **45** 2072–81

Li M *et al* 2017a Anthropogenic emission inventories in China: a review *Natl Sci. Rev.* **4** 834–66

Li M *et al* 2017b MIX: a mosaic Asian anthropogenic emission inventory under the international collaboration framework of the MICS-Asia and HTAP *Atmos. Chem. Phys.* **17** 935–63

Liu J *et al* 2016 Air pollutant emissions from Chinese households: a major and underappreciated ambient pollution source *Proc. Natl Acad. Sci.* **113** 7756–61

Long X, Tie X, Cao J, Huang R, Feng T, Li N, Zhao S, Tian J, Li G and Zhang Q 2016 Impact of crop field burning and mountains on heavy haze in the North China Plain: a case study *Atmos. Chem. Phys.* **16** 9675–91

Riahi K *et al* 2017 The shared socioeconomic pathways and their energy, land use, and greenhouse gas emissions implications: an overview *Glob. Environ. Change* **42** 153–68

Shen X and Liu B 2016 Changes in the timing, length and heating degree days of the heating season in central heating zone of China *Sci. Rep.* **6** 33384

Tao S *et al* 2018 Quantifying the rural residential energy transition in China from 1992 to 2012 through a representative national survey *Nat. Energy* **3** 567–73

Tong D *et al* 2020 Dynamic projection of anthropogenic emissions in China: methodology and 2015–2050 emission pathways under a range of socio-economic, climate policy, and pollution control scenarios *Atmos. Chem. Phys.* **20** 5729–57

Wang X, Lang X and Jiang D 2022 Detectable anthropogenic influence on summer compound hot events over China from 1965 to 2014 *Environ. Res. Lett.* **17** 034042

World Health Organization 2021 WHO global air quality guidelines: particulate matter (PM2.5 and PM10), ozone, nitrogen dioxide, sulfur dioxide and carbon monoxide (Geneva: World Health Organization)

Wu J and Gao X J 2013 A gridded daily observation dataset over China region and comparison with the other datasets *Chin. J. Geophys.* **56** 1102–11

Xiao Q, Ma Z, Li S and Liu Y 2015 The impact of winter heating on air pollution in China *PLoS One* **10** e0117311

Yuan S, Xu W and Liu Z 2015 A study on the model for heating influence on $PM_{2.5}$ emission in Beijing China *Proc. Eng.* **121** 612–20

Zhang Q *et al* 2019 Drivers of improved PM2.5 air quality in China from 2013 to 2017 *Proc. Natl Acad. Sci.* **116** 24463–9

Zhang W, Cui Y, Wang J, Wang C and Streets D G 2020a How does urbanization affect CO_2 emissions of central heating systems in China? An assessment of natural gas transition policy based on nighttime light data *J. Clean. Prod.* **276** 123188

Zhang W, Wang H, Zhang X, Peng Y, Zhong J, Wang Y and Zhao Y 2020b Evaluating the contributions of changed meteorological conditions and emission to substantial reductions of PM2.5 concentration from winter 2016–2017 in Central and Eastern China *Sci. Total Environ.* **716** 136892

Zhao B *et al* 2018 Change in household fuels dominates the decrease in PM2.5 exposure and premature mortality in China in 2005–2015 *Proc. Natl Acad. Sci. USA* **115** 12401–6

Zheng B *et al* 2018 Trends in China's anthropogenic emissions since 2010 as the consequence of clean air actions *Atmos. Chem. Phys.* **18** 14095–111